

Benefiting from the Unique Properties of Lanthanide Ions

JEAN-CLAUDE G. BÜNZLI*

École Polytechnique Fédérale de Lausanne (EPFL), Laboratory of Lanthanide Supramolecular Chemistry (LCSL), CH-1015 Lausanne, Switzerland

Received September 12, 2005

ABSTRACT

The recent upsurge of interest in contrast agents for magnetic resonance imaging, of luminescent chemosensors for medical diagnostic, and lately, for optical imaging of cells has generated an impressive momentum for the coordination and supramolecular chemistry of trivalent lanthanide ions. We shortly review the synthetic methods allowing the introduction of these spherical ions with fascinating optical and magnetic properties into elaborate mono- and polymeric edifices. We then illustrate these methods by selected examples describing the use of (i) a coronand to produce luminescent liquid crystals, (ii) derivatized calixarenes for 4f–5f element separation, (iii) podates for the production of nanoparticles with high relaxivity and for sensitizing the near-infrared (NIR) emission, and (iv) self-assembly processes for producing functional bimetallic edifices.

1. A Series of Astounding Elements

The 15 elements from lanthanum (atomic number 58) to lutetium (atomic number 71) are termed *lanthanides*;¹ they correspond to the gradual filling of the 4f electron shell, which is shielded by the outer 5s²5p⁶ subshells. All of the elements in the group have a close chemical resemblance, which rendered their separation and characterization quite difficult. Their discovery extended over more than a century (Ce, 1803; Lu, 1907; artificial Pm, 1947), and identification was very often primarily made by spectroscopy. Lanthanides have the general electronic configuration [Xe]4fⁿ5d¹6s² with $n = 0$ (La) to 14 (Lu), and their most stable oxidation state, particularly in water, is +3 with a [Xe]4fⁿ configuration, although a rich chemistry of their divalent state is now developing in nonaqueous solvents.¹ The technological importance of these elements for magnetic and optical materials, as well as for catalysts and additives in metallurgy, has long attracted interest in their physical properties and solid-state chemistry. The development of efficient separation technologies in the early 1960s, shift reagents for NMR spectroscopy in the 1970s, contrast agents for medical magnetic resonance

imaging in the early 1980s, luminescent chemosensors for medical diagnostics in the late 1980s,² and more recently optical imaging of cells³ have however gradually increased the interest for their solution and coordination chemistry. Moreover, lanthanides have also increasing utility in organic synthesis, bioorganic chemistry, and homogeneous catalysis.^{4–6} Incorporating a given Ln^{III} ion into molecular edifices with specific properties is not particularly easy in view of their poor steric requirements and of their similar chemical properties; some of them are gathered in Table 1. In fact, chemistry, spectroscopy, and magnetism of these ions differ considerably from d transition-metal ions in that ligand field effects are very small (a few hundred cm⁻¹ versus 5000–30 000 cm⁻¹), a reality not always well-assimilated by chemists. Because this Account is centered on the work published by our laboratory, which mostly deals with luminescence, we shall essentially focus on photophysical properties in the following description.

Lanthanide ions display three types of electronic transitions. First, the forbidden and faint intraconfiguration f–f transitions, with absorption coefficients smaller than 10 M⁻¹ cm⁻¹ (and often <1 M⁻¹ cm⁻¹).⁸ The corresponding transitions are quite narrow, and the barycenter of the ligand-field split bands does not depend much on the chemical environment of the ion. Therefore, these transitions are easily recognizable, making lanthanide ions ideal candidates for optical probes, especially that a thorough investigation of the splitting by group-theory considerations⁹ leads to precise information on the symmetry of the metal-ion environment. In addition, most of the ions are luminescent (see Figure 1), either fluorescent (e.g., Pr^{III}, Nd^{III}, Ho^{III}, Er^{III}, and Yb^{III}) or phosphorescent (e.g., orange Sm^{III}, red Eu^{III}, Gd^{III}, which emits in the UV, green Tb^{III}, yellow Dy^{III}, and blue Tm^{III}); their emission colors cover the entire spectrum from UV to visible and near-infrared (NIR) ranges (0.3–2.2 μm), and they are usually rather pure, so that they may be used in trichromatic phosphors for lighting purposes. Two ions, La^{III} and Lu^{III}, have no f–f transitions and are not luminescent. The second kind of transitions involves the promotion of a 4f electron into the 5d subshell (f–d transitions). These transitions are allowed, broader than f–f transitions, and their energy depends largely upon the metal environment because the 5d orbitals are external and interact directly with the ligand orbitals. For instance, Ce^{III} luminescence can be tuned from about 290 to 400 nm, depending upon the matrix that the ion is inserted into. The 4f–5d transitions have high energies (Figure 2),¹⁰ and only those of Ce^{III}, Pr^{III}, and Tb^{III} are commonly observed. Finally, charge-transfer transitions, both ligand-to-metal and metal-to-ligand, constitute the third kind of electronic transitions. Again, they are allowed, but their energies are high, so that only the LMCT of Eu^{III} and Yb^{III} (possibly Sm^{III} and Tm^{III}) are commonly observed, contrary to d transition-metal ions for which

* To whom correspondence should be addressed. E-mail: jean-claude.bunzli@epfl.ch.

Jean-Claude Bünzli is a physical-inorganic and analytical chemist by training and an active researcher in the field of coordination and supramolecular chemistry of the lanthanide ions. He earned a degree in chemical engineering in 1968 and a Ph.D. in 1971 from the école Polytechnique Fédérale de Lausanne (EPFL). He spent 2 years at the University of British Columbia and 1 year at the Swiss Federal Institute of Technology in Zürich before being appointed at the University of Lausanne in 1974. Since 2001, he has been a full professor of inorganic chemistry at EPFL. His research focuses mainly on the relationship between luminescent properties and the structure of lanthanide-containing molecular edifices, on the use of lanthanide ions as luminescent probes, and on the design of self-assembled building blocks for the synthesis of materials with predetermined photophysical and magnetic properties.

Table 1. Some Properties of the Lanthanides and Their Trivalent Ions

element	Ln	A ^a (μg g ⁻¹)	r _{at} ^b (pm)	E _{red} ⁰ ^b (V)	E _{red} ⁰ ^c (V)	R ₁ ^d (pm)	-ΔH _h ^{0e} (kJ mol ⁻¹)	-log* β ₁₁ ^f	log K (F ⁻) ^g	log K (dtpa) ^h	log K (dota) ⁱ	log k _{H₂O} ^j Ln(H ₂ O) _n	(^{2S+1})Γ _J (Ln ³⁺) ^k	μ _{eff} ^l (Ln ³⁺)
lanthanum	La	18.0	187	-2.522	-3.1	121.6	3326	9.01	2.67	19.48	22.86	na	¹ S ₀	0
cerium	Ce	46.0	182	-2.483	-3.2	119.6	3380	10.6	2.81	20.33	23.39	na	² F _{5/2}	2.3–2.5
praseodymium	Pr	6.0	182	-2.462	-2.7	117.9	3421	8.55	3.01	21.07	23.01	na	³ H ₄	3.4–3.6
neodymium	Nd	24.0	182	-2.431	-2.6 ^l	116.3	3454	8.43	3.09	21.60	22.99	na	⁴ I _{9/2}	3.5–3.6
promethium	Pm			-2.423		114.4	3482					na	⁵ L ₄	(2.68) ⁿ
samarium	Sm	6.5	180	-2.414	-1.55 ^m	113.2	3512	8.34	3.12	22.34	23.04	na	⁶ H _{5/2}	1.4–1.7
europium	Eu	1.0	200	-2.407	-0.35 ^m	112.0	3538	8.31	3.19	22.39	23.45	na	⁷ F ₀	3.3–3.5
gadolinium	Gd	6.5	180	-2.397	-3.9	110.7	3567	8.35	3.31	22.46	24.67	8.92	⁸ S _{7/2}	7.9–8.0
terbium	Tb	1.0	178	-2.391	-3.7	109.5	3600	8.16	3.42	22.71	24.22	8.75	⁷ F ₆	9.5–9.8
dysprosium	Dy	4.5	177	-2.353	-2.5 ^l	108.3	3634	8.10	3.46	22.82	24.79	8.64	⁶ H _{15/2}	10.4–10.6
holmium	Ho	1.0	177	-2.319	-2.9	107.2	3663	8.04	3.52	22.78	24.54	8.33	⁵ I ₈	10.4–10.7
erbium	Er	2.5	175	-2.296	-3.1	106.2	3692	7.99	3.54	22.74	24.43	8.12	⁴ H _{15/2}	9.4–9.6
thulium	Tm	0.1	174	-2.278	-2.3 ^l	105.2	3717	7.95	3.56	22.72	24.41	7.96	³ H ₆	7.1–7.5
ytterbium	Yb	2.5	194	-2.267	-1.15 ^m	104.2	3740	7.92	3.58	22.20	25	7.67	² F _{7/2}	4.3–4.9
lutetium	Lu	0.9	173	-2.255		103.2	3759	7.90	3.61	22.44	25.41	na	¹ S ₀	0

^a Abundance in earth crust. ^b Ln³⁺(aq) + 3 e⁻ D Ln. ^c Ln³⁺ + e⁻ D Ln²⁺, calculated values, otherwise stated. ^e Ionic radius for Ln³⁺ and a coordination number of 9. ^e Hydration enthalpies. ^f Hydrolysis constants, log* β₁₁ = [Ln(OH)²⁺]/[H⁺][Ln³⁺]. ^g Stability constants of the complexes with fluoride. ^h Stability constants of the complexes with diethylenetriaminopentaacetic acid (dtpa). ⁱ Stability constants of the complexes with dota (1,4,7,10-tetraazacyclododecane-1,4,7,10-tetraacetic acid). ^j Water exchange rate (aquo ions). ^k Electronic ground level. ^l Effective paramagnetic magnetic moment in compounds. ^m In THF. ⁿ In water. ⁿ Calculated value.

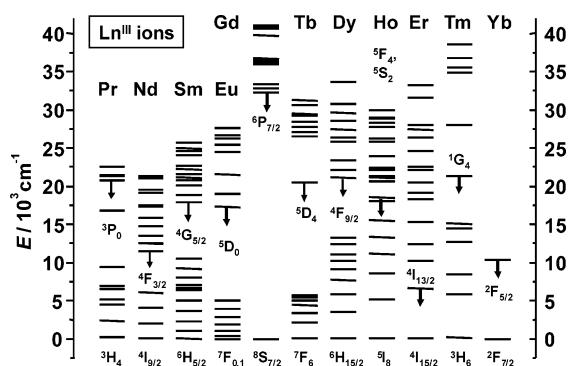


FIGURE 1. Partial energy diagrams⁸ of lanthanide trivalent ions (except La, Ce, Pm, and Lu) showing the ground state and one of the most luminescent excited states (for a given ion, several excited states are usually luminescent, except for Gd and Yb).

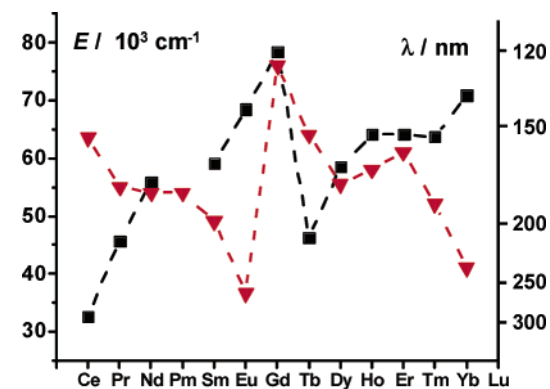


FIGURE 2. Energy of the 4f → 5d transitions of Ln^{III} ions in a CaF₂ matrix (■) and of the 2p(O) → 4f ligand-to-metal charge-transfer transitions (LMCT, red ▼). The right vertical axis bears a wavelength scale for the sake of convenience.

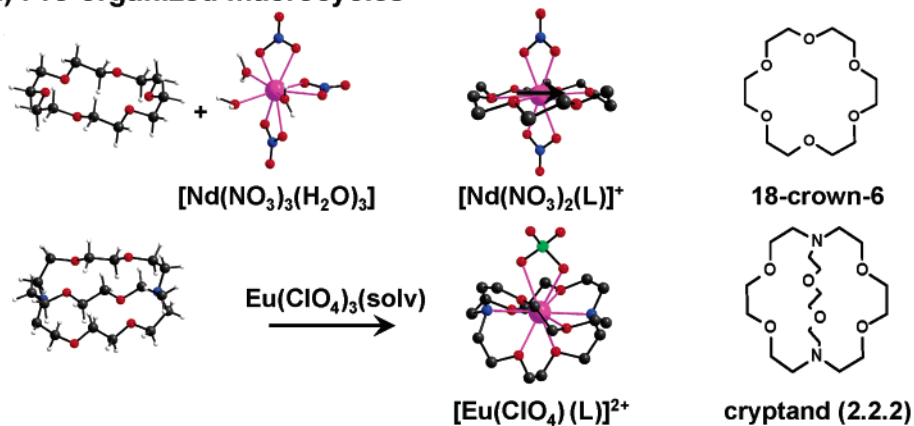
this type of transition is widespread. This information is not well-assimilated, so that one sometimes sees emission spectra of lanthanide coordination compounds wrongly assigned to LMCT, by analogy to d metal complexes. As an example, the calculated 2p(O)–4f transitions are displayed in Figure 2.¹¹

2. Designing Lanthanide-Containing Functional Edifices

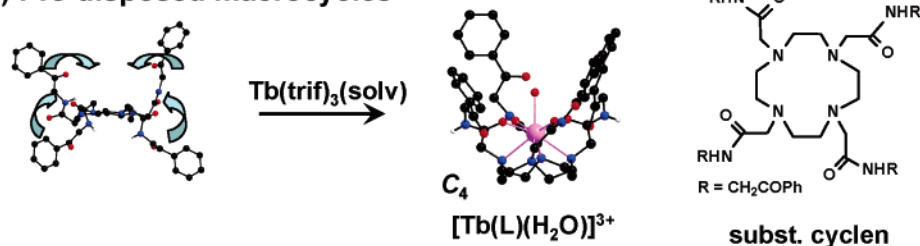
In aqueous solutions, the enthalpy and entropy changes upon complex formation between Ln^{III} cations and many ionic ligands is predominantly influenced by changes in the hydration of both the cation and ligand(s). Complexation results in a decrease in the hydration, yielding a positive entropy change favorable to the complexation process. On the other hand, dehydration is endothermic and the contribution from bond formation between the cation and ligand(s) often does not compensate this unfavorable energy contribution to the variation in Gibbs free energy, so that the overall complexation process is generally entropy-driven. Therefore, it is advantageous to resort to polydentate ligands for building a coordination environment around Ln^{III} ions and benefit from the chelate effect, especially when forming the edifices in water, because the hydration enthalpies of the Ln^{III} ions are rather large (Table 1). The crucial idea is to take control of the coordination sphere and, henceforth, to gain a handle on the electronic properties of the Ln^{III} ions. The following points ought to be addressed.

(a) Except if some special effects are planned, one looks for a saturation of the inner coordination sphere. Contrary to d transition-metal complexes, coordination numbers (CN) are usually large in the absence of sizable steric hindrance, in the range of 6–12 with a predominance for CN 8–10 (CN as small as 3 or 4 are obtained with bulky ligands, e.g., bis(trimethylsilyl)amide [N(SiMe₃)₂]⁻ or bis(isopropyl)amide).¹² The ligand must therefore possess an adequate number of donor atoms, otherwise solvent molecules will complete the coordination sphere, unless a ternary donor such as bipyridine or phenanthroline is added. Water molecules in the inner coordination sphere deactivate the Ln^{III} excited states nonradiatively and quench the luminescence. On the other hand, they are indispensable to MRI experiments and very useful when responsive analytical luminescent sensors are developed.²

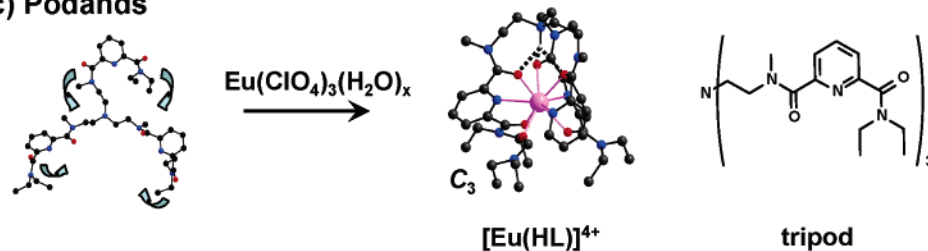
a) Pre-organized macrocycles



b) Pre-disposed macrocycles



c) Podands



d) Self-assembly processes

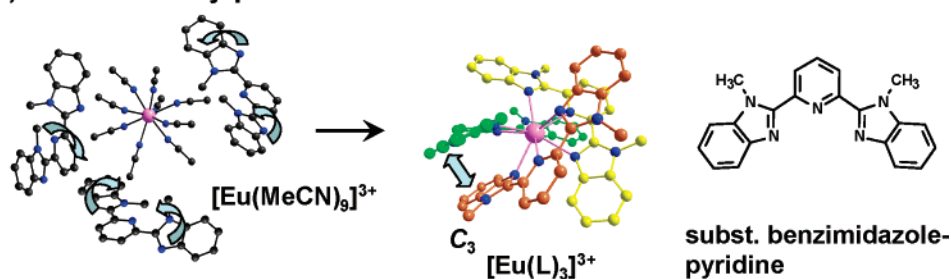


FIGURE 3. Synthetic strategies used to insert lanthanide ions into molecular edifices. All reactions are carried out in acetonitrile. The following structures were redrawn from literature data: $[\text{Nd}(\text{NO}_3)_3(\text{H}_2\text{O})_3]$,²² $[\text{Nd}(\text{NO}_3)_2(18\text{C}6)]^+$,²³ $[\text{Eu}(\text{ClO}_4)(2.2.2.)]^{2+}$,²⁴ $[\text{Tb}(\text{L})(\text{H}_2\text{O})]^{3+}$,¹⁵ $[\text{Eu}(\text{HL})]^{4+}$,¹⁸ $[\text{Eu}(\text{MeCN})_9]^{3+}$,²⁵ and $[\text{Eu}(\text{L})_3]^{3+}$.²⁶ Other structures were optimized by the PM3 procedure (CAche Work System Pro 6.1, from Fujitsu).

(b) The strength of the Ln–ligand interaction has to be maximized. Because Ln^{III} ions are rather hard cations, with chemical bonds having a large electrostatic components, anionic ligands will be preferred, which bear either oxygen- or nitrogen-donor atoms. Aminocarboxylates or β -diketonates are widely used anionic ligands, which yield thermodynamically stable complexes.

(c) The size of the resulting chelating ring has also an influence, in that five-membered rings result in more stable complexes.

(d) Ln^{III} ions are highly labile (Table 1), which may be detrimental to some *in vivo* applications. One should

therefore look for ligands yielding kinetically stable edifices (e.g., cyclen derivatives).

In view of the weak steric requirement of the lanthanide ions, several strategies have been developed over the past decades for the design of mono- and polymetallic lanthanide-containing molecular and polymeric assemblies. In addition to classical polydentate chelating agents (e.g., polyaminocarboxylates and β -diketonates), these approaches include the use of (i) macrocyclic receptors, either preorganized, e.g., crown ethers or cryptands, or predisposed, e.g., large macrocycles or cyclen derivatives and calixarenes fitted with functionalized pendant arms,¹³ (ii) podands, or (iii) self-assembly processes (Figure 3).¹⁴

Following the lines of the *Lock and Key principle*, preorganized receptors such as coronands or cryptands have been designed to encapsulate given metal ions. These receptors have the same conformation in the free and bound states, which minimize the reorganization work upon complexation. The recognition process simply relies on the match between the cavity size and the metal-ion diameter. The ionic radius of Ln^{III} ions varies only slightly along the series [$\Delta r_i(\text{La-Lu}) \approx 0.18 \text{ \AA}$ for coordination number 9; Δr_i between consecutive Ln^{III} ion is in the range of 0.01–0.02 \AA]. A molecular programming matching exactly the size of one ion is almost impossible to achieve. Although Ln^{III} complexes with preorganized receptors have been synthesized (Figure 3a) and characterized, their stability, particularly in water, has been somewhat deceptive and coordination chemists have soon turned to predisposed macrocycles (Figure 3b). The latter (e.g., cyclen¹⁵ or calixarene derivatives¹⁶) bear functionalized pendant arms that wrap around the metal ion, forming an induced cavity (so-called *Induced Fit Principle*). Although the conformational work upon complexation is larger than with preorganized receptors, it is more than compensated by the enthalpy gain in host–guest interaction,¹⁷ and the complexes with 1,4,7,10-tetraaza-cyclododecane-*N,N,N',N''*-tetraacetic acid (dota) rank among the most stable Ln^{III} coordination compounds ($p\text{Ln} \approx 21\text{--}22$) ($p\text{Ln} = -\log[\text{Ln}^{\text{III}}(\text{aq})]^{3+}$ when $[\text{Ln}^{\text{III}}]_t = 10^{-6} \text{ M}$ and $[\text{ligand}] = 10^{-5} \text{ M}$, at pH 7.4). When the design of the functionalized edifice requires the presence of bidentate or tridentate arms, their attachment onto relatively large macrocycles is sometimes difficult to carry out, so that in a further simplifying step they can simply be grafted onto smaller anchors: tetra-armed receptors are often built from aromatic rings (e.g., benzene), while the functional groups of tri-armed ligands are attached on a single atom, nitrogen, boron, or a transition-metal ion. The advantage of podands is that the number and nature of donor atoms can easily be varied. On the other hand, because they are less predisposed than the pendant arm-fitted macrocycles, the correct orientation of the arms upon complexation requires more work. A way out of this difficulty is to resort to weak noncovalent interactions, such as hydrogen bonding, to organize the arms, so that the donor atoms are positioned in a favorable way. This is depicted in Figure 3c, in which rare trifurcated hydrogen bonding maintains the three coordinating units of the receptor in the adequate spatial conformation for an optimum interaction with the Ln^{III} ions.¹⁸ Self-assembly processes are a major tool in molecular recognition and supramolecular chemistry. The key to self-assembly in coordination chemistry is that, in addition to strong ion–dipole interactions, the formation of the host cavity relies on the presence of programmed weak noncovalent interactions between the ligand strands. This is illustrated in Figure 3d, where the three benzimidazole moieties are spatially organized by the nine Ln–N ion–dipole bonds and by interstrand π – π interactions between almost parallel aromatic rings. Application of the same principle using bicompartamental, penta-, or hexadentate receptors has led

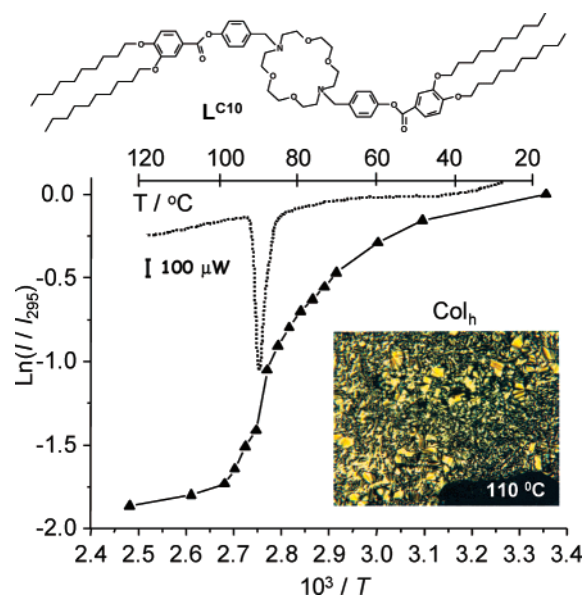


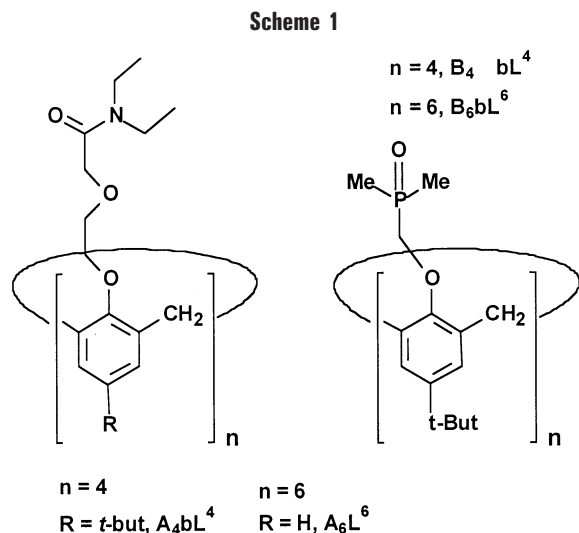
FIGURE 4. S-shaped variation of the luminescence intensity of $[\text{Eu}(\text{NO}_3)_3(\text{L}^{\text{C}10})]$ versus $1/T$ with, in a dotted line, the corresponding differential scanning calorimetric curve. The inset shows a polarized light microscopy view of the hexagonal columnar phase. Redrawn from ref 31.

to the isolation by strict self-assembly of stunning 3d–4f, 4f–4f, or 4f–4f⁺ bimetallic helicates,¹⁴ while further extension to nonadentate receptors allowed the synthesis of 4f–4f–4f homo-¹⁹ and heterotrimetallic²⁰ helicates. Rational modeling of the assembly of these helicates is now at hand,²¹ so that self-assembly processes slowly emerge as a privileged strategy for the engineering of elaborate multimetallic edifices and devices. In the following sections, we shall describe selected examples from our work with coronands, calixarenes, podands, and self-assembly processes.

3. Calixarene- and Coronand-Based Macrocyclic Chemistry

A Derivatized Coronand for Generating Luminescent Metallomesophases. The present interest in the design and study of lanthanide-containing mesophases²⁷ is justified by several potential applications in bioanalyses and materials sciences. There are basically two strategies for designing lanthanide-containing liquid crystals, which have been known since 1977.²⁷ The first, simpler one consists of doping lanthanide salts or complexes, for instance, the highly luminescent β -diketonates, in known cholesteric and nematic phases. We have also exploited the remarkable properties of room-temperature ionic liquids, with some of them displaying mesogenic phases.^{28,29} In the other approach, specific ligands are synthesized, which lead to mesomorphic lanthanide complexes.³⁰

On the basis of our experience in lanthanide macrocyclic chemistry, we have designed a series of promesogenic ligands derived from the known coronand 1,10-diaza-4,7,13,16-tetraoxacyclooctadecane, abbreviated (2,2). Macrocycle $\text{L}^{\text{C}10}$ (Figure 4) is nonmesomorphic, but its complexes with lanthanide nitrates display a columnar



hexagonal liquid crystalline phase, as proven by small-angle X-ray diffraction measurements.³¹ In the case of $[Eu(\text{NO}_3)_3L^{C10}]$, this mesophase extends from 85 to 195 °C. Additionally, we were able to demonstrate that luminescence parameters such as intensity and lifetime vary in a S-shape fashion during the crystalline-to-liquid crystalline transition (Figure 4), so that they are useful for an easy determination of the transition temperature.³¹

Derivatized Calixarenes for Ln/An Separation. Calixarenes act as versatile blocks in supramolecular and coordination chemistry, because both of their wider (lower) and narrower (upper) rims can be easily derivatized to induce specific functionalities. In the past years, we have developed model calixarenes for the study of energy migration mechanisms in polymetallic compounds and of 4f–4f magnetic interactions.³² More recently, we have designed two series of branched calixarenes having 4f–5f separation capabilities while being good sensitizers of the Ln^{III} luminescence: one bearing ether-amide pendant arms ($A_n bL^n$, $n = 4$ and 6; see Scheme 1) and a second one fitted with phosphinoyl groups ($B_n bL^n$, $n = 4, 6$, and 8). The ether-amide A substituent acts as a bidentate coordinating unit forming (stable) five-membered chelate rings upon binding to the metal ion. In solution, $A_4 bL^4$ adopts a cone conformation with a time-averaged C_{4v} symmetry, and its 1:1 complexes with Ln^{III} ions are stable in acetonitrile ($\log K_1 = 9.6$ for La). The crystal structure of the Lu complex points to the four ligand arms wrapping around the metal ion, forming a protective cavity that is rigidified by the presence of one water molecule, bound to the metal ion and hydrogen-bonded to the phenolic oxygen atoms (Figure 5).¹⁶ The formation of these hydrogen bonds offsets the entropic disadvantage of relatively long pendant arms, which have to organize themselves around the metal ion. Characteristic metal-centered luminescence is observed upon excitation into the ligand levels, with quantum yields in acetonitrile remaining modest (2% for Eu and 5.8% for Tb).

When the calixarene framework is enlarged and simultaneously the *tert*-butyl groups are removed in A_6L^6 , the

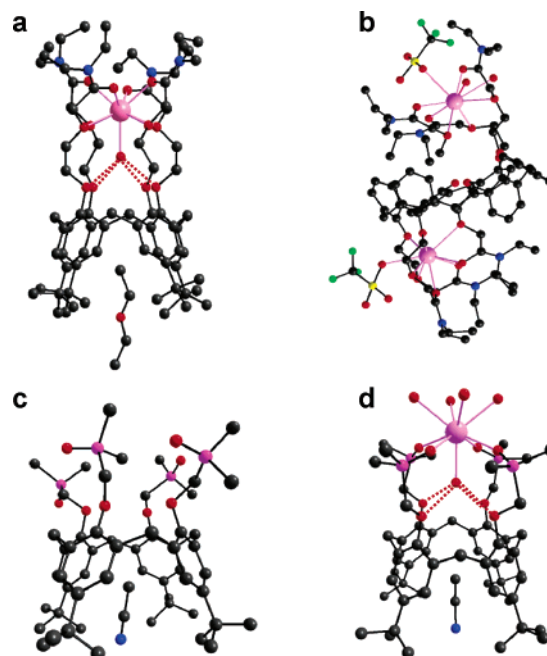


FIGURE 5. Redrawn crystal structures of (a) $\{[\text{Lu}(\text{A}_4\text{bL}^4)(\text{H}_2\text{O})] \cdot 2\text{Et}_2\text{O}\}^{3+}$,¹⁶ (b) $[\text{Eu}_2(\text{OTf})_2(\text{A}_6\text{L}^6)(\text{H}_2\text{O})_2]^{4+}$ (calculated structure),³³ (c) $\text{B}_4\text{bL}^4 \cdot \text{MeCN}$,³⁴ and (d) $\{[\text{La}(\text{B}_4\text{bL}^4)(\text{H}_2\text{O})_5]\} \cdot \text{MeCN}$ (unpublished result). Hydrogen bonds shaping the cavities are indicated with dotted red lines.

situation changes considerably. Conformational interconversion is much easier, and the formation of 2:1 (Ln/L) complexes is favored. Molecular mechanics calculations taking into account solvent effects show the conformer with the lowest energy displaying a pinched “chair” conformation of the 1,2,3-alternate type. Experimentally, this is substantiated by NMR data in solution and by the isolation of a bimetallic complex with Eu, $[\text{Eu}_2(\text{OTf})_2(\text{A}_6\text{L}^6)(\text{H}_2\text{O})_2]^{4+}$, the calculated structure of which is shown in Figure 5.³³ Its quantum yield in acetonitrile (2.5%) is comparable to the one mentioned above for the 1:1 complex with A_4bL^4 .

Macrocyclic $B_n bL^n$ also adopts a cone conformation, both in the solid state and in solution.³⁴ The phosphinoyl substituent has a stronger donor strength than the ether-amide moiety, resulting in a larger stability of the 1:1 and 1:2 complexes in acetonitrile: $\log \beta_1 = 11.4 \pm 1.5$, and $\log \beta_2 = 19.6 \pm 1.8$ ($\text{Ln} = \text{La}$). An interesting point is that a different structure is obtained for 1:1 complexes depending upon their hydration. When the complex is hydrated, the lanthanide ion lies on top of the cavity and is solely coordinated to the four phosphinoyl groups, in addition to five water molecules. Upon dehydration, the lanthanide ion lowers into the cavity formed by the pendant arms and the phenolic groups of the receptor are coordinated as well. The phenomenon is reversible, leading to a push–pull movement upon addition or removal of water.

According to its crystal structure, the larger receptor B_6bL^6 adopts a distorted alternate *in–out* cone conformation, with adjacent phenyl rings being almost perpendicular. It also yields 1:1 and 1:2 complexes in acetonitrile with trivalent Ln ions, with a stability comparable to the one exhibited by the complexes with the calix[4]arene

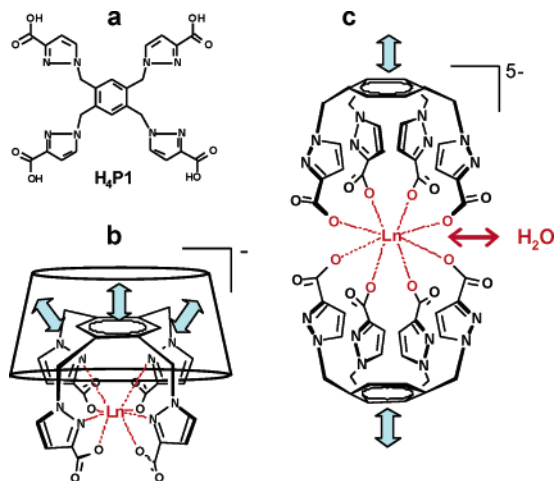


FIGURE 6. Tetrapodal ligand (a), interaction of its 1:1 chelate with cyclodextrin (b), and sketch of the 1:2 podate (c).

derivative and somewhat improved photophysical properties (quantum yields for the Eu solutions, 1.5–2.5%).

In summary, the two series of macrocyclic receptors present remarkable characteristics with respect to Ln^{III} ion complexation. The stoichiometry of the corresponding complexes can be tuned by a suitable choice of the narrower and/or wider rim substituents. With the calix-[4]arenes adopting a cone conformation, induced cavities can be formed through hydrogen bonding with coordinated water molecules. The Eu^{III} and Tb^{III} complexes are luminescent enough to present some analytical interest, despite their modest quantum yields. Presently, extraction studies are in progress with the B_nLⁿ series of ligands.

4. The Podand Approach

Self-Aggregated Nanoparticles for Magnetic Resonance Imaging (MRI). In an effort to develop a system with luminescent properties and displaying powerful contrast agent capability for MRI, we have turned to nanometric particles. Podand H₄P1 was engineered to match the following requirements. First, it should be able to strongly coordinate Ln^{III} ions, and the resulting chelates should be amenable to association through a noncovalent intermolecular interaction to yield ternary complexes with potential carriers such as cyclodextrins or to self-aggregate into stable nanoparticles (Figure 6). The benzene ring anchor is meant to generate soft intermolecular interactions, while pyrazole groups are known to be good sensitizers of the lanthanide luminescence.³⁵ The podand interacts with lanthanide ions in water, yielding 1:1 and 1:2 podates with sizable stability ($\log \beta_1 \approx 13$ and $\log \beta_2 \approx 23$, and $pLn \approx 9-10$). The 1:1 podates further react with cyclodextrins ($\log K_{11} = 6.0$ for β -CD in water, Figure 6b), and the resulting Tb^{III} ternary complexes display a 4-fold enhancement of their metal-centered luminescence compared with the parent podate. Solutions of the 1:2 podates (Figure 6c) become turbid at a concentration larger than 3×10^{-5} M, revealing self-aggregation. A careful study of the resulting Gd^{III} particles by several experimental techniques point to the formation of two types of spherical

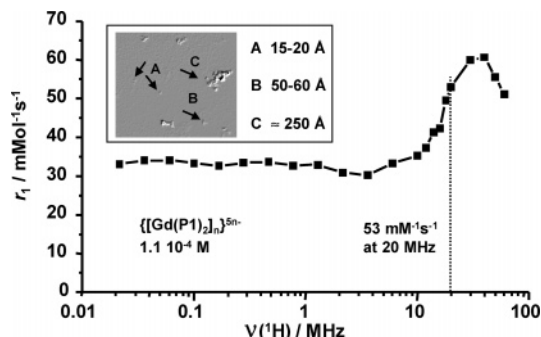


FIGURE 7. NMRD profile of $\{Gd(P1)_2\}_n^{5n-}$ particles at 25 °C and pH 7.2. The inset features a pseudo-3D transmission electron micrograph of the particles collected on an Au grid. Redrawn from ref 35.

nanoparticles with mean radii of 11 ± 1 nm (A) and 57 ± 15 nm (B, Figure 7). The critical aggregation concentrations were determined to be 3×10^{-5} M and 10^{-4} M. Above the latter concentration, the spherical nanoparticles coagulate into much larger aggregates with ill-defined morphology (C). Stacking of the podates via their anchor is suggested by NMR and allows the nanoparticles to minimize electrostatic repulsion. The good colloidal stability of the spherical particles also results from charge compensation, probably through H_3O^+ or K^+ ions, as demonstrated by electrophoretic mobility and ζ potential measurements.³⁵ The striking property of the spherical Gd^{III} nanoparticles lies in their large relaxivity (Figure 7). The high-field peak in the range of 20–60 MHz is consistent with a slow rotational correlation time and large rigidity of the system. The relaxivity observed at 25 °C is about 13 times larger than the one exhibited by the well-known commercial contrast agent $[Gd(dota)]^-$ (DOTAREM). ¹⁷O NMR titration of the Dy^{III} analogue and excited-state lifetimes of the Eu^{III} and Tb^{III} podates point to an average of 2–3 water molecules interacting with each lanthanide ion. Further experiments have shown that the nanoparticles display good resistance toward exchange with Zn^{II} and no cytotoxicity; on the other hand, kinetic tests show too great a lability, so that the nanoparticles will have to be stabilized before becoming potential contrast agents.³⁶

Sensitizing the NIR Emission of Ln^{III} Ions. During the past decade, *in vivo* optical detection of tumors by means of NIR photons has gained momentum because it represents a noninvasive technique, allowing the exploration of deeper tissues, with the investigation range extending from a few millimeters up to 20 cm.³⁷ Indeed, biological tissues have very low absorption coefficients above 700 nm, and in addition, the absorption of water, a major component of biological tissues, diminishes drastically above 900 nm. Until now, most of these clinical applications have made use of organic dyes as probes for NIR imaging, and differentiation between the target and background fluorescence has been achieved by molecular switches activated *in vivo* by a suitable biochemical reaction. An alternate strategy would be to resort to bioprobes incorporating NIR-emitting lanthanide ions³ such as Nd^{III}, with fluorescence lines in three distinct

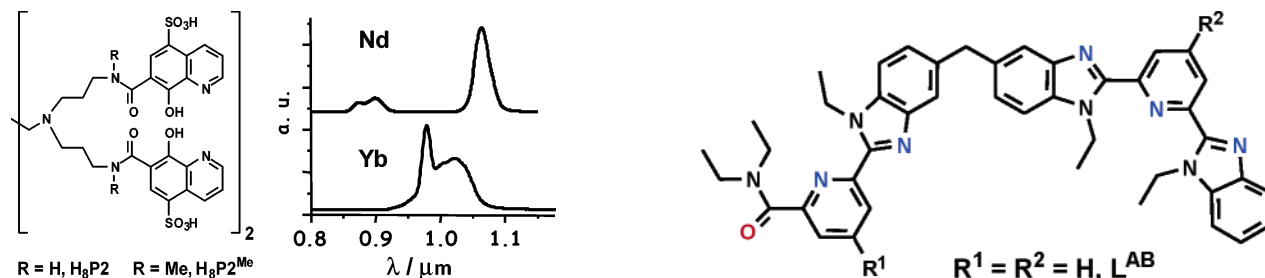


FIGURE 8. Formulas of the podands designed for sensitizing the luminescence of the NIR emitting Ln^{III} ions and part of the emission spectra of 6×10^{-5} M [Ln(H₂P2)]³⁻ in water, at pH 7.4 and room temperature.⁴⁰

spectral ranges: 0.87–0.92, 1.06–1.09, and 1.32–1.39 μm ($^4\text{F}_{3/2} \rightarrow ^4\text{I}_{9/2}$, $^4\text{I}_{11/2}$, and $^4\text{I}_{13/2}$ transitions) or Yb^{III}, which gives off light in the range of 0.98–1.03 μm ($^2\text{F}_{5/2} \rightarrow ^2\text{F}_{7/2}$ transition). With respect to the visible-emitting Ln^{III} ions, those displaying NIR luminescence have two intrinsic drawbacks: (i) comparatively shorter lifetimes (from nano- to microseconds), which somewhat limit the efficiency of time-resolved experiments, and (ii) they are more amenable to nonradiative deactivation, because of a smaller energy gap between their emissive and ground states. The first disadvantage can be overcome by the use of d transition-metal ions for the population of the excited states of the 4f ions.^{38,39} We have recently developed a strategy to address the second problem, by designing podands based on a short 1,2-diaminoethane backbone fitted with four 8-hydroxyquinoline moieties because the corresponding anion is known to be an efficient sensitizer of Ln^{III} NIR luminescence. The spacer bears an amide coupling function, and its length has been chosen to achieve a tight coordination environment around the Ln^{III} ion (Figure 8).⁴⁰

The chelate effect obtained with H₈P2 is impressive, with pLn values of [Ln(H₂P2)]³⁻ being in the range of 15–16, compared with ≈ 8 for [Ln(8-hydroxyquinolate)]₃. Moreover, lifetime determination of the Ln excited states clearly proves the absence of water in the inner coordination sphere, resulting in quantum yields, which, for Yb^{III}, are among the largest reported for a molecular species in water: 0.18 and 0.37% for [Yb(H₂P2)]³⁻ and [Yb(H₂P2^{Me})]³⁻, respectively.⁴⁰

5. Self-Assembly Processes

During the last 15 years, we have synthesized several ditopic ligands that self-assemble with Ln^{III} and/or d transition-metal ions to yield bimetallic 4f–4f and 3d–4f edifices with predetermined luminescent or magnetic properties. Stable homobimetallic 4f–4f helicates have been assembled both in acetonitrile^{41–43} and water,⁴⁴ and the mechanism of the self-assembly process leading to the exclusive formation of these triple-stranded bimetallic helicates has been elucidated using a fruitful combination of electrospray mass spectrometry, potentiometry, UV–vis spectrophotometry, luminescence, and ¹H NMR.⁴⁵

In parallel, we have devoted a large synthetic effort to produce hexadentate unsymmetrical ligands, with two

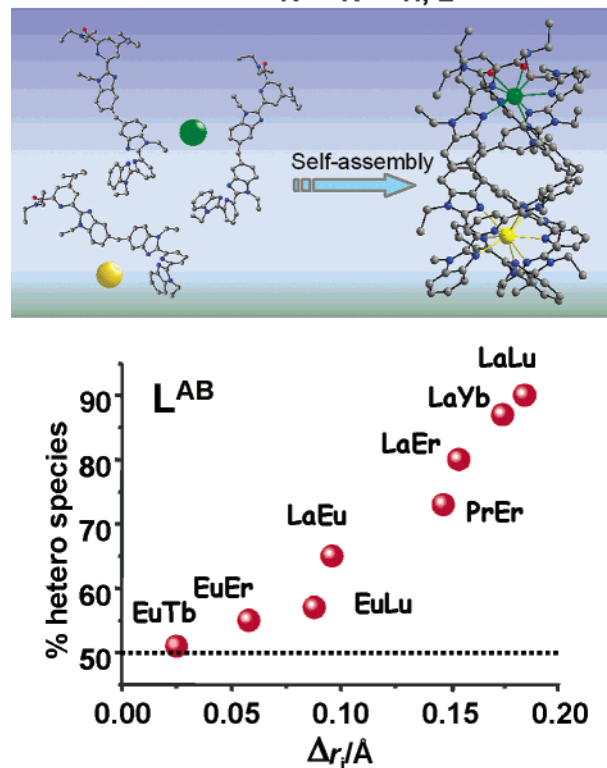


FIGURE 9. Heteroditopic ligand L^{AB} (top) leading to the isolation of heterobimetallic 4f–4f' helicates (middle). The percentage of hetero species is reported at the bottom (from NMR and ES–MS data).⁴⁶

coordination units of different strength, in an attempt to recognize heteropairs of lanthanide ions (Figure 9). Altogether, remarkable enhancements in the concentration of the heterobimetallic [LnLn'(L^{AB})₃]⁶⁺ species over the statistical distribution are obtained when the ionic radius difference is larger than 0.1 Å, reaching up to 90% for the LaLu pair (Figure 9).⁴⁶ In terms of energy, this translates into differences in ΔG_r (with respect to the statistical situation) remaining modest, between -3 and -10 kJ mol⁻¹, henceforth the difficulty in planning the adequate ligands. It is noteworthy that the softer tridentate unit, bis(benzimidazolylpyridine), is always bound to the larger (softer) lanthanide ion, as ascertained by several crystal-structure determinations and NMR data. The quantum yields of the LaEu, EuEu, and EuLu species in acetonitrile are reasonable,⁴⁷ so that luminescent probes derived from these helicates can be envisaged. Presently, we are investigating the subtle origins of the selectivity toward a given hetero pair of Ln^{III} ions by modulating the coordinating strength of the tridentate units by means of substituents R¹ and R². A good understanding of these origins will allow

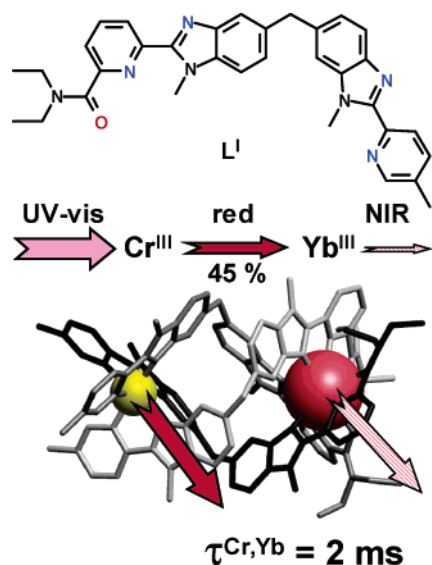


FIGURE 10. Heteroditopic ligand L^1 (top) leading to the isolation of heterobimetallic Cr–Ln helicates (bottom) acting as directional nanometric light-converting devices and in which the luminescent properties of the Yb^{III} ion are controlled by the 3d metal ion.^{38,39}

chemists to master the design of ingenious hosts, leading to functional bimetallic edifices.

In collaboration with Prof. C. Piguet, many 3d–4f helicates have been investigated¹⁴ and one striking example is the control of the Nd^{III} and Yb^{III} luminescent properties, particularly their apparent lifetime, through Cr^{III} or Ru^{II} . Dependent upon the kinetic regime associated with each specific d–f pair, the NIR luminescence decay times can be tuned from micro- to milliseconds by the population of the Ln^{III} excited levels through directional $Cr^{III} \rightarrow Ln^{III}$ energy transfer (Figure 10).^{38,39}

6. Conclusion

The various examples described above illustrate the wide variety of potential applications that lanthanides may have in the field of coordination chemistry. The main lesson emerging from the numerous papers published in the field during the past decade is that synthetic procedures are presently well-mastered, so that lanthanide-containing edifices can be designed with all of the required physicochemical properties, both as molecular compounds or coordination polymers⁴⁸ obtained by crystal engineering. Modeling is also progressing, but the ultimate *ab initio* design of, say, highly luminescent lanthanide-containing stains is not yet within reach, given the various parameters involved in the energy transfer. However, the promising topic of NIR-emitting probes will certainly have a positive impact on the field. Finally, the availability of ditopic ligands able to self-assemble with a hetero pair of lanthanides ions opens the way for fascinating polymetallic functional edifices.

The author thanks the past and present collaborators of his research group for their important experimental input as well as the Swiss National Science Foundation and the Swiss Federal Office for Science and Education for financial support (COST action D18).

References

- (1) Evans, W. J. Perspectives in Reductive Lanthanide Chemistry [Review]. *Coord. Chem. Rev.* **2000**, *206*, 263–283.
- (2) Bünzli, J.-C. G.; Piguet, C. Taking Advantage of Luminescent Lanthanide Ions. *Chem. Soc. Rev.* **2005**, *34*, 1048–1077.
- (3) Faulkner, S.; Pope, S. J. A.; Burton-Pye, B. P. Lanthanide Complexes for Luminescence Imaging Applications. *Appl. Spectrosc. Rev.* **2005**, *40*, 1–31.
- (4) Edmonds, D. J.; Johnston, D.; Procter, D. J. Samarium(II)-Iodide-Mediated Cyclizations in Natural Product Synthesis. *Chem. Rev.* **2004**, *104*, 3371–3403.
- (5) Komiyama, M. Cutting DNA and RNA. In *Handbook on the Physics and Chemistry of Rare Earths*; Gschneidner, K. A. Jr., Bünzli, J.-C. G., Pecharsky, V. K., Eds.; Elsevier B. V.: Amsterdam, The Netherlands, 2004; Vol. 34, Chapter 222.
- (6) Molander, G. A.; Romero, J. A. C. Lanthanocene Catalysts in Selective Organic Synthesis. *Chem. Rev.* **2002**, *102*, 2161–2186.
- (7) Helm, L.; Merbach, A. E. Inorganic and Bioinorganic Solvent Exchange Mechanisms. *Chem. Rev.* **2005**, *105*, 1923–1960.
- (8) Carnall, W. T. The Absorption and Fluorescence Spectra of Rare Earth Ions in Solution. In *Handbook on the Physics and Chemistry of Rare Earths*; Gschneidner, K. A. Jr., Eyring, L., Eds.; North-Holland: Amsterdam, The Netherlands, 1979; Vol. 3, Chapter 24.
- (9) Bünzli, J.-C. G. Rare Earth Luminescent Centers in Organic and Biochemical Compounds. In *Spectroscopic Properties of Rare Earths in Optical Materials*; Liu, G. K., Jacquier, B., Eds.; Springer-Verlag: Berlin, Germany, 2005; Vol. 83, Chapter 11.
- (10) Dorenbos, P. f → d Transition Energies of Divalent Lanthanides in Inorganic Compounds. *J. Phys.: Condens. Matter* **2003**, *15*, 575–594.
- (11) Shionoya, S.; Yen, W. M. Principal Phosphor Materials and Their Optical Properties. In *Phosphor Handbook*; Shionoya, S., Yen, W. M., Eds.; CRC Press, Inc.: Boca Raton, FL, 1999; Chapter 3.
- (12) Bünzli, J.-C. G. Coordination Chemistry of the Trivalent Lanthanide Ions: An Introductory Overview. In *Rare Earths*; Saez Puche, R., Caro, P., Eds.; Editorial Complutense: Madrid, Spain, 1998.
- (13) Bünzli, J.-C. G. Complexes with Synthetic Ionophores. In *Handbook on the Physics and Chemistry of Rare Earths*; Gschneidner, K. A., Jr., Eyring, L., Eds.; Elsevier Science Publisher: Amsterdam, The Netherlands, 1987; Vol. 9, Chapter 60.
- (14) Bünzli, J.-C. G.; Piguet, C. Lanthanide-Containing Molecular and Supramolecular Polymetallic Functional Assemblies. *Chem. Rev.* **2002**, *102*, 1897–1928.
- (15) Zucchi, G.; Ferrand, A.-C.; Scopelliti, R.; Bünzli, J.-C. G. Highly Luminescent, Visible-Emitting Lanthanide Macrocyclic Chelates Stable in Water and Derived from the Cyclen Framework Lanthanide Chelates Based on Cyclen Derivatives. *Inorg. Chem.* **2002**, *41*, 2459–2465.
- (16) Ramirez, F. d. M.; Charbonnière, L. J.; Muller, G.; Scopelliti, R.; Bünzli, J.-C. G. A *p*-*tert*-Butyl[4]arene Functionalised at Its Lower Rim with Ether-Amide Pendant Arms Acts as Inorganic/Organic Receptor: Structural and Photophysical Properties of Its Lanthanide Complexes. *Dalton Trans.* **2001**, 3205–3213.
- (17) Sastri, V. S.; Bünzli, J.-C. G.; Rao, V. R.; Rayudu, G. V. S.; Perumareddi, J. R. *Modern Aspects of Rare Earths and Complexes*; Elsevier B. V.: Amsterdam, 2003; Chapter 4B, pp 303–375.
- (18) Renaud, F.; Piguet, C.; Bernardinelli, G.; Bünzli, J.-C. G.; Hopfgartner, G. Nine-Coordinate Lanthanide Podates with Predetermined Structural and Electronic Properties: Facial Organization of Unsymmetrical Tridentate Binding Units by a Protonated Covalent Tripod. *J. Am. Chem. Soc.* **1999**, *121*, 9326–9342.
- (19) Floquet, S.; Ouali, N.; Bocquet, B.; Bernardinelli, G.; Imbert, D.; Bünzli, J.-C. G.; Hopfgartner, G.; Piguet, C. The First Self-Assembled Trimetallic Lanthanide Helicates Driven by Positive Cooperativity. *Chem.–Eur. J.* **2003**, *9*, 1860–1875.
- (20) Floquet, S.; Borkovec, M.; Bernardinelli, G.; Pinto, A.; Leuthold, L.-A.; Hopfgartner, G.; Imbert, D.; Bünzli, J.-C. G.; Piguet, C. Programming Heterotrimetallic Lanthanide Helicates: Thermodynamic Recognition of Different Metal Ions along the Strands. *Chem.–Eur. J.* **2004**, *10*, 1091–1105.
- (21) Piguet, C.; Borkovec, M.; Hamacek, J.; Zeckert, K. Strict Self-Assembly of Polymetallic Helicates: The Concepts behind the Semantics. *Coord. Chem. Rev.* **2005**, *249*, 705–729.
- (22) Jones, C.; Junk, P. C.; Smith, M. K.; Thomas, R. C. Identification of the Structural Boundary between $[Ln(18\text{-Crown-6})(NO_3)_3]$ and $[Ln(NO_3)_3(H_2O)_3] \cdot 18\text{-Crown-6}$ Motifs in the Lanthanide Series. *Z. Anorg. Allg. Chem.* **2000**, *626*, 2491–2497.
- (23) Bünzli, J.-C. G.; Klein, B.; Wessner, D.; Schenk, K. J.; Chapuis, G.; Bombieri, G.; De Paoli, G. Crystal and Molecular Structure of the 4:3 Complex of 18-Crown-6 Ether with Neodymium Nitrate. *Inorg. Chim. Acta* **1981**, *54*, L43–L46.

- (24) Ciampolini, M.; Dapporto, P.; Nardi, N. Structure and Properties of Some Lanthanoid(III) Perchlorates with the Cryptand 4,7,13-, 16,21,24-Hexaoxa-1,10-diazabicyclo[8.8.8]hexacosane. *J. Chem. Soc., Dalton Trans.* **1979**, 974.
- (25) Deacon, G. B.; Gortler, B.; Junk, P. C.; Lork, E.; Mews, R.; Petersen, J.; Zemva, B. Syntheses and Structures of Some Homoleptic Acetonitrile Lanthanoid(III) Complexes. *J. Chem. Soc., Dalton Trans.* **1998**, 3887–3891.
- (26) Piguet, C.; Williams, A. F.; Bernardinelli, G.; Bünzli, J.-C. G. Structural and Photophysical Properties of Lanthanide Complexes with Planar Aromatic Tridentate Nitrogen Ligands as Luminescent Building Blocks for Triple-Helical Structures. *Inorg. Chem.* **1993**, *32*, 4139–4149.
- (27) Binnemans, K.; Görlner-Walrand, C. Lanthanide Containing Liquid Crystals and Surfactants. *Chem. Rev.* **2002**, *102*, 2303–2345.
- (28) Guillet, E.; Imbert, D.; Scopelliti, R.; Bünzli, J.-C. G. Tuning the Emission Color of a Mesogenic Ionic Liquid Doped with Eu^{III} Salts. *Chem. Mater.* **2004**, *16*, 4063–4070.
- (29) Puntus, L.; Bünzli, J.-C. G. Intense Near-Infrared Luminescence of a Mesomorphic Ionic Liquid Doped with Lanthanide B-Diketates. *Eur. J. Inorg. Chem.* **2005**, 4739–4744.
- (30) Terazzi, E.; Suárez, S.; Torelli, S.; Nozary, H.; Imbert, D.; Mamula, O.; Rivera, J.-P.; Guillet, E.; Benech, J.-M.; Bernardinelli, G.; Scopelliti, R.; Donnio, B.; Guillon, D.; Bünzli, J.-C. G.; Piguet, C. Introducing Bulky Functional Lanthanide Cores into Thermotropic Metallomesogens: A Bottom-to-Top Approach. *Adv. Funct. Mater.* **2005**, in press.
- (31) Suárez, S.; Imbert, D.; Gummy, F.; Piguet, C.; Bünzli, J.-C. G. Metal-Centered Photoluminescence as a Tool for Detecting Phase Transitions in Eu^{III}- and Tb^{III}-Containing Metallomesogens. *Chem. Mater.* **2004**, *16*, 3257–3266.
- (32) Bünzli, J.-C. G.; Besançon, F.; Ihringer, F. Bimetallic Lanthanide Supramolecular Edifices with Calixarenes. In *Calixarenes for Separations*; Lumetta, G. J., Rogers, R. D., Gopalan, A., Eds.; American Chemical Society: Washington, DC, 2000; Vol. 757, Chapter 14.
- (33) Ramirez, F. d. M.; Charbonnière, L. J.; Muller, G.; Bünzli, J.-C. G. Tuning the Stoichiometry of Lanthanide Complexes with Calixarenes: Bimetallic Complexes with a Calix[6]arene Bearing Ether–Amide Pendant Arms. *Eur. J. Inorg. Chem.* **2004**, 2348–2355.
- (34) Le Saulnier, L.; Varbanov, S.; Scopelliti, R.; Elhabiri, M.; Bünzli, J.-C. G. Lanthanide Complexes with a *p*-*tert*-Butylcalix[4]arene Fitted with Phosphinoyl Pendant Arms. *J. Chem. Soc., Dalton Trans.* **1999**, 3919–3925.
- (35) Fatin-Rouge, N.; Tóth, E.; Perret, D.; Backer, R. H.; Merbach, A. E.; Bünzli, J.-C. G. Lanthanide Podates with Programmed Inter-molecular Interactions: Luminescence Enhancement through Association with Cyclodextrins and Unusually Large Relaxivity of the Gadolinium Self-Aggregates. *J. Am. Chem. Soc.* **2000**, *122*, 10810–10820.
- (36) Fatin-Rouge, N.; Tóth, E.; Meuli, R.; Bünzli, J.-C. G. Enhanced Imaging Properties of a Gd^{III} Complex with Unusually Large Relaxivity. *J. Alloys Compd.* **2004**, *374*, 298–302.
- (37) Weissleder, R.; Ntziachristos, V. Shedding Light onto Live Molecular Targets. *Nat. Med.* **2003**, *9*, 123–128.
- (38) Torelli, S.; Imbert, D.; Cantuel, M.; Bernardinelli, G.; Delahaye, S.; Hauser, A.; Bünzli, J.-C. G.; Piguet, C. Tuning the Decay Time of Lanthanide-Based near Infrared Luminescence from Micro- to Milliseconds through d–f Energy Transfer in Discrete Heterobimetallic Complexes. *Chem.–Eur. J.* **2005**, *11*, 3228–3242.
- (39) Imbert, D.; Cantuel, M.; Bünzli, J.-C. G.; Bernardinelli, G.; Piguet, C. Extending Lifetimes of Lanthanide-Based NIR Emitters (Nd, Yb) in the Millisecond Range through Cr^{III} Sensitization in Discrete Bimetallic Edifices. *J. Am. Chem. Soc.* **2003**, *125*, 15698–15699.
- (40) Imbert, D.; Comby, S.; Chauvin, A.-S.; Bünzli, J.-C. G. Lanthanide 8-Hydroxyquinoline Based Podates with Efficient Emission in the NIR Range. *Chem. Commun.* **2005**, 1432–1434.
- (41) Piguet, C.; Bünzli, J.-C. G.; Bernardinelli, G.; Hopfgartner, G.; Williams, A. F. Self-Assembly and Photophysical Properties of Lanthanide Dinuclear Triple-Helical Complexes. *J. Am. Chem. Soc.* **1993**, *115*, 8197–8206.
- (42) Martin, N.; Bünzli, J.-C. G.; McKee, V.; Piguet, C.; Hopfgartner, G. Self-Assembled Dinuclear Lanthanide Helicates: Substantial Luminescence Enhancement upon Replacing Terminal Benzimidazole Groups by Carboxamide Binding Units. *Inorg. Chem.* **1998**, *37*, 577–589.
- (43) Gonçalves e Silva, F. R.; Malta, O. L.; Reinhard, C.; Güdel, H. U.; Piguet, C.; Moser, J. E.; Bünzli, J.-C. G. Visible and Near-Infrared Luminescence of Lanthanide-Containing Dimetallic Triple-Stranded Helicates: Energy Transfer Mechanisms in the Sm^{III} and Yb^{III} Molecular Edifices. *J. Phys. Chem. A* **2002**, *106*, 1670–1677.
- (44) Elhabiri, M.; Scopelliti, R.; Bünzli, J.-C. G.; Piguet, C. Lanthanide Helicates Self-Assembled in Water: A New Class of Highly Stable and Luminescent Dimetallic Carboxylates. *J. Am. Chem. Soc.* **1999**, *121*, 10747–10762.
- (45) Elhabiri, M.; Hamacek, J.; Bünzli, J.-C. G.; Albrecht-Gary, A.-M. Lanthanide Homodimetallic Triple-Stranded Helicates: Insight into the Self-Assembly Mechanism. *Eur. J. Inorg. Chem.* **2004**, 51–62.
- (46) André, N.; Jensen, T. B.; Scopelliti, R.; Imbert, D.; Elhabiri, M.; Hopfgartner, G.; Piguet, C.; Bünzli, J.-C. G. Supramolecular Recognition of Heteropairs of Lanthanide Ions: A Step toward Self-Assembled Bifunctional Probes. *Inorg. Chem.* **2004**, *43*, 515–529.
- (47) Jensen, T. B. Design of Lanthanide Heterobimetallic Helicates. Ph.D. Thesis, in progress, 2006; Swiss Federal Institute of Technology Lausanne (EPFL), Lausanne, Switzerland.
- (48) Guillou, O.; Daiguebonne, C. Lanthanide-Containing Coordination Polymers. In *Handbook on the Physics and Chemistry of Rare Earths*; Gschneidner, K. A., Jr., Bünzli, J.-C. G., Pecharsky, V. K., Eds.; Elsevier North-Holland: Amsterdam, The Netherlands, 2004; Vol. 34, Chapter 221.

AR0400894